Computational identification of natural product leads that inhibit mast cell chymase: an exclusive plausible treatment for Japanese encephalitis

Kamal Kant, Ravi Rawat, Vipin Bhati, Shailesh Bhosale, Dalchand Sharma, Subham Banerjee & Anoop Kumar

View supplementary material

Accepted author version posted online: 10 Feb 2020.
Published online: 18 Feb 2020.

Submit your article to this journal

Article views: 53

View related articles

View Crossmark data

Check for updates

Computational identification of natural product leads that inhibit mast cell chymase: an exclusive plausible treatment for Japanese encephalitis

Kamal Kant[a,b], Ravi Rawat[c†], Vipin Bhati[d], Shailesh Bhosale[d], Dalchand Sharma[e], Subham Banerjee[a,b] and Anoop Kumar[d]

[a]Department of Pharmaceutics, National Institute of Pharmaceutical Education and Research (NIPER), Guwahati, Assam, India; [b]National Centre for Pharmacoengineering, National Institute of Pharmaceutical Education and Research (NIPER), Guwahati, Assam, India; [c]Department of Pharmaceutical Sciences and Technology, Birla Institute of Technology, Mesra, Ranchi, Jharkhand, India; [d]Department of Pharmacology and Toxicology, National Institute of Pharmaceutical Education and Research (NIPER), Raebareli, Uttar Pradesh, India; [e]Regional Centre for Biotechnology, Faridabad, Haryana, India
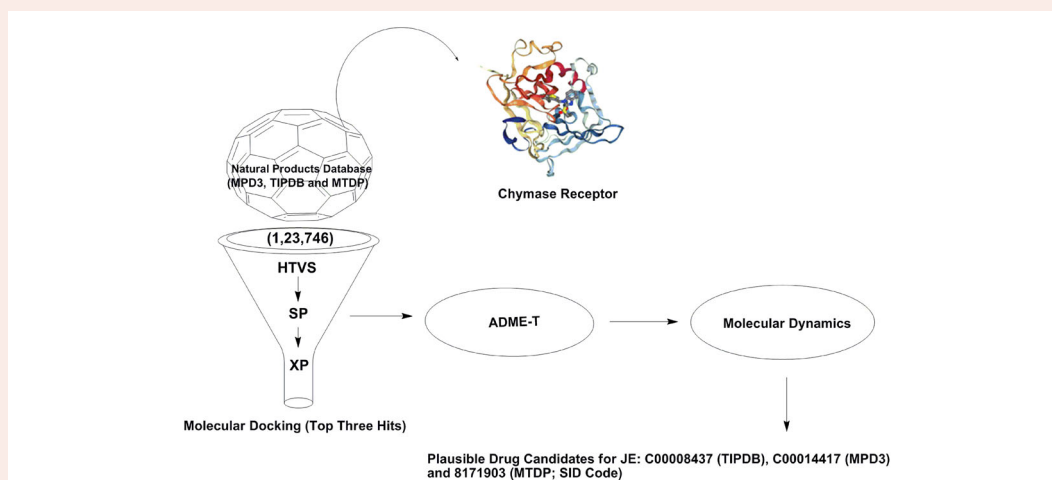
Communicated by Ramaswamy H. Sarma

ABSTRACT

A recent research has identified chymase, a mast cell-specific protease as an exclusive novel therapeutic target to prevent Japanese encephalitis virus (JEV) induced encephalitis. Interestingly, JEV activates mast cell specific chymase during its penetration through blood brain barrier (BBB) which eventually guide to viral encephalitis. Hence, in this study, natural chemical entities (NCE) from multiple databases (MPD3, TIPDB and MTDP) were virtually screened for their binding affinity as chymase inhibitors, a promising negotiator for prolong survival against JEV tempted encephalitis. Merged computational programs, Maestro software, QikProp, ProTox and Gromacs were applied to screen the NCEs against target receptor (PDB: 4KP0). Three hits (C00008437, C00014417 and 8141903) were identified after employing a series of sieves such as High Throughput Virtual Screening (HTVS), Standard precision (SP) and Xtra precision (XP) molecular docking simulations followed by desired pharmacokinetic-toxicity profile predictions and molecular dynamics (MD) examinations. Maestro simulations resulted in best three binding energy scores as −11.992 kcal/mol (first ranked; C00008437), −11.673 kcal/mol (second ranked; C00014417) and −11.456 kcal/mol (third ranked; 8141903), respectively. The top three hits revealed an ideal range of pharmacokinetic and toxicity descriptors values. In addition, MD simulations enabled us to confirm top hits higher selectivity toward chymase receptor. In conclusion, this might potentially represent remarkable novel classes with an effective chymase mediated treatment to combat JEV induced encephalitis, which need to justify with further detail studies.

Natural Products Database (MPD3, TIPDB and MTDP)

Chymase Receptor

(1,23,746)

HTVS → SP → XP

Molecular Docking (Top Three Hits)

ADME-T → Molecular Dynamics

Plausible Drug Candidates for JE: C00008437 (TIPDB), C00014417 (MPD3) and 8171903 (MTDP; SID Code)

Abbreviations: ADME-T: absorption, distribution, metabolism and excretion-toxicity; AOFA: amine oxidase (flavin-containing) A; BBB: blood brain barrier; FOSA: hydrophobic component of the SASA; GROMACS: Groningen MAchine for Chemical Simulation; HTVS: high throughput virtual screening; JE: Japanese encephalitis; JEV: Japanese encephalitis virus; MD: molecular dynamics; MW: molecular weight; NCE: new chemical entities; PDB: Protein Data Bank; PGH1: prostaglandin G/H synthase 1;

1. Introduction

Japanese encephalitis (JE), originated from Japanese encephalitis virus (JEV), is a fatal neuroinflammatory disease affecting a large number of populations globally. Japanese encephalitis virus belongs to the family Flaviviridae (flavivirus) and transmit its virus cycle between mosquitoes (*Culex tritaeniorhynchus*) and humans (Arumugam et al., 2017; Bhimaneni & Kumar, 2020). This neurotropic virus is enveloped, icosahedral with positive sense single-stranded RNA viruses that cross the blood brain barrier (BBB) of host cells to cause JE in humans (Solomon et al., 2000). Japanese encephalitis is mostly established in the Asian and some parts of the Western pacific regions (Hills et al., 2019). As per World Health Organization (WHO) report, approximately 68,000 people are infected from JE every year, with a death rate of 15,000 people annually. Especially, 4,633 cases of JE with a mortality of 200 people are reported in 2008 from Western pacific regions (Campbell et al., 2011). In India, JE is more prevalent in Uttar Pradesh, West Bengal, Bihar, Tamil Nadu and North-eastern states (Kulkarni, Sapkal, Kaushal, & Mourya, 2018; McNaughton, Singh, & Khan, 2018). The common symptoms are ranged from headache, photophobia and neurological disorders. Notably, around half of the survivors from JE are even associated with neurological problems, muscle weakness, learning difficulties, and paralysis. Currently, there is no specific treatment approved for JE in preventing the development of neurological signs. However, only supportive and symptomatically management is the preferable option and infact their mechanisms are too poorly understood. The mechanism for JEV entry to central nervous system (CNS) gateway is unclear to date. The CNS is recognized immune loaded and is separated from peripheral tissues through BBB. Previous studies have indicated this hematological route (BBB) for JEV ingress into the brain in both human and mouse postmortem brain samples (Johnson et al., 1985; Liu, Liang, Wang, Liu, & Chen, 2008). Another *in vivo* study supports the JEV-induced breakdown of tight junction proteins between brain endothelial cells which ultimately lead to production of inflammatory cytokines and chemokines (Li et al., 2015). Although, hypothetical guess to have an immune factor concern and still remains a big question mark during JEV pathogenesis. Mast cells (MCs) are one of the important occupant immune cells in central nervous system, located near the BBB and the neurovascular unit (brain endothelial cells, pericytes, neurons, astrocytes, and microglia) (Khalil et al., 2007). Once MCs provoked by JEV or certain pathogens, it led to granular production comprised of inflammatory mediators, vasoactive molecules, proteases chymase and other chemical mediators (cytokines, chemokines and eicosanoids) (Abraham, Shwetank, & Manjunath, 2011). Recently, one report identified the MC-specific protease (Chymase), an important target for BBB mediated JEV neuroinvasion to reverse vascular outflow, limit virus and sustain survival (Hsieh, Rathore, Soundarajan, & John, 2019). Chymase can also act as a precursor for activating potent proteases like matrix metalloproteinase (MMP) −2 and −9, which in turns can augment the endothelial cell permeability and boost BBB disintegration. Although, several anti-JE synthetic drugs are explored but due to their non selectivity, inappropriate outcome and toxicity, now scientific communities have beared hope for breakthrough from natural origin (Kant, Walia, Agnihotri, Pathania, & Singh, 2013; Lv et al., 2018). Moreover, phytoconstituents namely arctigenin and rosmarinic acid illustrated marked reduction in JEV-induced neuronal cell death, microglial actuation and active caspase activity (Ghosh & Basu, 2009). Thus, in the current investigation, we have screened natural product derived inhibitors against human chymase receptor employing *in silico* approaches. The top hits identified in this study acts as a latest template for the potential treatment of JE.

2. Material and methods

Virtual screening methods such as High Throughput Virtual Screening (HTVS), Standard Precision (SP) and Xtra Precision (XP) protocols were applied using Maestro software 2019-3 (Schrödinger, LLC, Cambridge, USA). Pharmacokinetic parameters viz. absorption, distribution, metabolism and excretion-toxicity (ADME-T) were estimated with the aid of QikProp and Protox gadgets. The Dell brand system was used for molecular docking studies with a specification of i7 6700 socket LGA 1151 processor (3.40 GHz; 8 GB RAM) 64-bit equipped CENT OS Linux operating system. Molecular dynamics simulations were run on the ubuntu 14.04 LTS supported by 8 GB RAM employing GROMACS 5.0 program (Groningen MAchine for Chemical Simulation).

2.1. In silico study

2.1.1. Selection and refinement of human chymase protein
The reported structure of human chymase receptor was retrived from Protein Data Bank (PDB) with PDB ID of 4KP0. The resolution of human chymase was indicated as 2.8 Å having R-value free and work are 0.330 and 0.226, respectively. The internal ligand namely 4-({1-[(4-methyl-1-benzothiophen-3-yl)methyl]-1H-benzimidazol-2-yl}sulfanyl)butanoic acid (TJK002) was found to co-crystallize with the target protein (PDB ID: 4KP0). Retrive structure was downloaded in PDB format and exported into the Maestro software (Schrödinger, LLC, Cambridge, USA). Target protein structure was visualized through Maestro operating environment. Protein refinement was mediated by insertion of processing, optimization, and minimization steps indicated in protein preparation wizard.

Table 1. H-bonding and hydrophobic interactions of top three hits (entire screened databases) against chymase receptor (PDB: 4KP0).

Compounds	Gscore (kcal/mol)	H-bond (HBD[a] or HBA[a]) distance Å with allied Amino acid	Hydrophobic interactions (amino acid residues)
C00008437 (TIPDB)	−11.992	1.76-HBD (PHE41) 2.02-HBD 1.80-HBD (ALA190) 2.00-HBD 1.81-HBA (ARG143)	PHE41, ALA190, CYS42, PHE191, ALA226, VAL213, TYR215 and LEU99
C00014417 (MPD3)	−11.673	1.92-HBD (PHE41) 2.08-HBD 1.97-HBD (ALA190) 1.86-HBA (ARG143)	PHE41, CYS42, ALA226, PHE91, ALA190, TYR215 and VAL213
8141903 (MTDP; pubchem SID)	−11.456	1.72-HBA (GLY193) 2.17-HBA (SER195)	PHE41 and TYR215
Marketed reference (Nelfinavir)	−6.558		
Internal reference (4-({1-[(4-methyl-1-benzothiophen-3-yl)methyl]-1H-benzimidazol-2-yl}sulfanyl)butanoic acid)	−4.940	1.74-HBD (ALA190)	ALA190, VAL227, ALA226, VAL213, PHE191, TYR215, LEU99, CYS42, PHE41

[a]Ligand as hydrogen bond donor (HBD)/hydrogen bond acceptor (HBA).
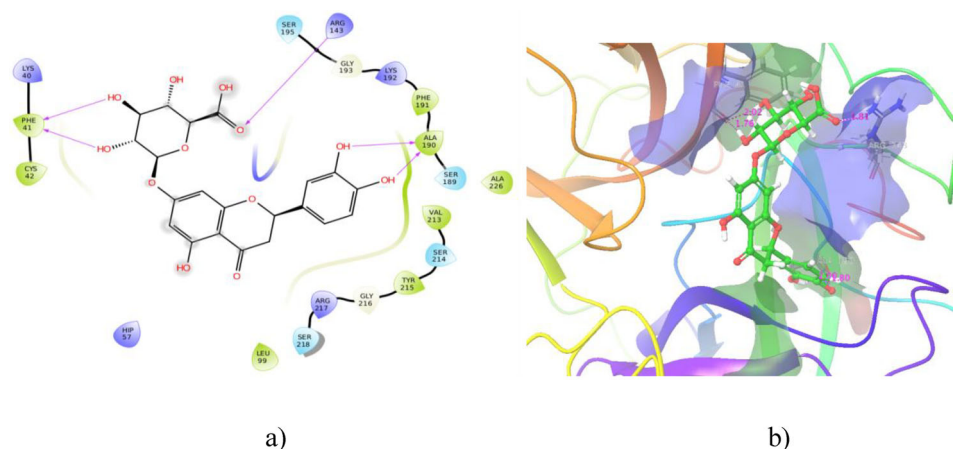
Figure 1. Docked C00008437 in complex (a: 2D and b: 3D) with chymase pocket (PDB: 4KP0) from TIPDB database.
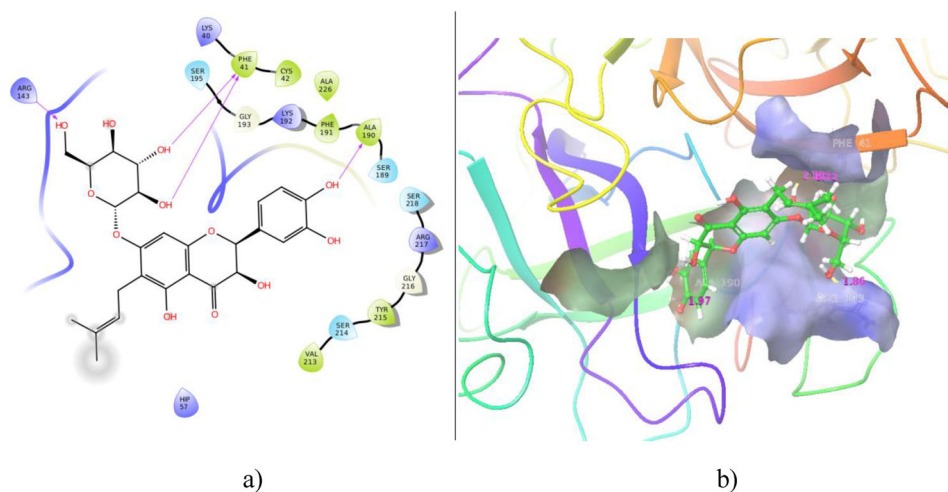
Figure 2. Docked C00014417 in complex (a: 2D and b: 3D) with chymase pocket (PDB: 4KP0) from MPD3 database.

Initially, proton insertions, bond order assignment followed by crystallographic water deletion (outside 5 Å) steps were applied. Other strides such as pH ionization, optimization, and energy minimization were too included to receive proper geometry of target receptor (Kant, Lal, Kumar, & Ghosh, 2019).

2.1.2. Ligand database preparation
An exhaustive literature was carried out to investigate the natural product based metabolites for activity against chymase mediated JE infection. Chemical structures of these metabolites were downloaded from MPD3 record, MTDP

a)   b)
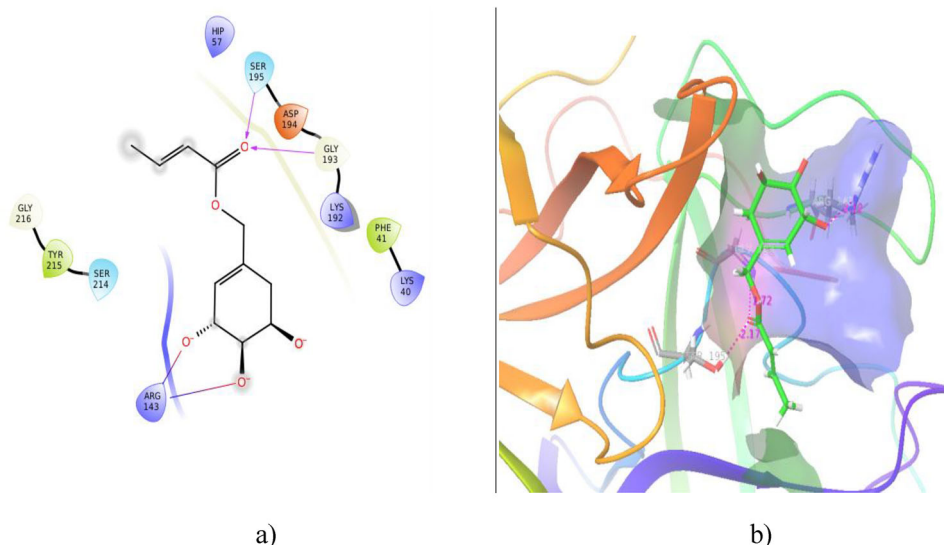
Figure 3. Docked 8142044 (pubchem SID) in complex (a: 2D and b: 3D) with chymase pocket (PDB: 4KP0) from MTDP database.

catalogue and TIPDB database in .sdf and mol2 formats. The low energy 3D conformation of ligands was executed with the support of LigPrep using OPLS 2005 force field. The ionization states were also adjusted prior to molecular docking simulation (Kumar, Behera, Rangra, Dey, & Kant, 2018).

2.1.3. Molecular docking

Maestro suite (Schrödinger, LLC, Cambridge, USA) was used to dock a different ligand database of natural product metabolites within the defined docking site (internal ligand) of human chymase receptor (PDB: 4KP0). Particularly, the receptor grid was generated by specifying the internal ligand of target receptor. Glide's docking algorithm was applied to scrute best poses of docked molecules. The different conformers of tested ligands were minimized through force field refinement algorithm in which ultimately binding energy is calculated in form of glide score (Gscore). The apex hits were ranked on the basis of Gscore and Root-Mean-Square Deviation (RMSD) values (Halgren et al., 2004). From the apex hits, scheme was to choose merely those entities for advance investigation that bind to active residues of human chymase receptor with noteworthy dock score. Already descripted internal ligand was redocked as reference ligand with the human chymase protein to validate molecular docking procedure employed to predict the natural product metabolites within the active site pocket.

2.1.4. Ligand-receptor interaction examination

For better understanding of ligand-receptor interaction, the best docked complexes 2-D plots of ligand interactions were examined through Ligplot tool of Maestro suite (Halgren et al., 2004). It includes a 2D plot of H-bonding, hydrophobic interactions, Pi-Pi stacking and Pi-cation etc. which contributes the affinity of drug like entities within the active site of JEV human chymase receptor. 3-D plots of top hits inhibitor complexes were included using Maestro suite.

2.1.5. ADME-T inspect

In silico estimation of top hits for drug likeliness was calculated with pharmacokinetic descriptors as indicated in QikProp tool. Toxicity assessment of these apex hits was predicted using Protox server. Various target pathways such as hepatotoxicity, immunotoxicity, mutagenicity and cytotoxicity were evaluated (Drwal, Banerjee, Dunkel, Wettig, & Preissner, 2014; Ioakimidis, Thoukydidis, Mirza, Naeem, & Reynisson, 2008). The ADME-T profile was judged to minimize drug failure rate during drug discovery process.

2.1.6. Molecular dynamics simulation

Molecular dynamics (MD) simulation was used for the optimization of ligand protein complex by imitating the real physiological environment (Rana, Sharma, & Kumar, 2019). The best top docked complexes were predicted to molecular dynamics (MD) simulations to confirm their strong binding affinity and encouraging molecular interaction network. The top hits docked complexes and control apo structutre of chymase protein were compared to MD simulation using GROMACS 5.0 suite and GROMOS9643a1 force field. Explicit solvent MD simulation and topology framework of protein and top hit ligands were built using GROMACS 5.0 and Dundee Prodrg 2.5 tools. Ligand-receptor complexes were solvated in hexagonal box via 3-site rigid water molecule with charges and Lennard-Jones parameters assigned to each of the 3 atoms. Long range electrostatics (Particle Mesh Ewald) and short range van-der Waals were calculated with defined parameters. The system was stabilized under NVT ensemble by gradually increasing the temperature from 0 K to 300 K. Following, the system was adjusted with pressure (1 bar) and temperature (300 K) under NPT ensemble. Periodic boundary stipulation was carried out with the help of atomic constraints of the system with an energy description of 10.0 PS (Jacob et al. 2017; Kant et al., 2019; Van Der Spoel et al., 2005). Ultimately, 100 ns production run was executed and coordinates of the system were saved after each 2 fs for further analysis. The trajectory

Table 2. Assessment of pharmacokinetic descriptors for top hits using QikProp.

Compounds	MW	Dipole†	SASA	FOSA	PISA	QPpolrz	QPlogPoct‡	QPlogS	QPlogBB	QPlogKhsa	Lipinski's rule of five
C00008437	464.382	10.317	706.361	104.092	194.961	40.022	29.442	−3.53	−4.273	−0.849	2
C00014417	534.516	6.714	817.920	290.224	156.87	47.722	35.225	−3.795	−4.276	−0.724	3
8141903 (MTDP; pubchem SID)	228.244	3.684	500.118	265.349	43.313	23.237	15.652	−2.253	−1.576	−0.642	0

Data signified: MW, molecular weight; Dipole†, dipole moment; SASA, total solvent accessible surface area (SASA) in square ang-stroms using a probe with a 1.4 Å radius; FOSA, hydrophobic component of the SASA; PISA, π (carbon and attached hydrogen) component of the SASA; QPpolrz, predicted polarizability in cubic angstroms; QPlogPoct‡, predicted octanol/gas partition coefficient; QPlogS, predicted aqueous solubility; QPlogBB, predicted brain/blood partition coefficient; QPlogKhsa, prediction of binding to human serum albumin.

Table 3. Prediction of the toxicity parameters for apex entities using ProTox.

Chemical entities	Toxicity class (LD_{50} mg/kg)	Hepatotoxicity (probable value)	Carcinogenicity (probable value)	Mutagenicity (probable value)	Cytotoxicity (probable value)	Probable toxicity targets
C00008437	5 (2300)	Inactive (0.74)	Inactive (0.60)	Inactive (0.68)	Inactive (0.60)	AOFA, PGH1
C00014417	5 (2300)	Inactive (0.73)	Inactive (0.83)	Inactive (0.64)	Inactive (0.68)	AOFA, PGH1
8141903 (MTDP; pubchem SID)	5 (2600)	Inactive (0.77)	Inactive (0.83)	Inactive (0.80)	Inactive (0.81)	AOFA, PGH1

Data designated: toxicity class; Class 1, fatal if swallowed ($LD_{50} \leq 5$ mg/kg); Class 2, fatal if swallowed ($5 < LD_{50} \leq 300$ mg/kg); Class 3, toxic if swallowed ($50 < LD_{50} \leq 300$ mg/kg); Class 4, harmful if swallowed ($300 < LD_{50} \leq 2000$ mg/kg); Class 5, may be harmful if swallowed ($2000 < LD_{50} \leq 5000$ mg/kg); Class 6, non-toxic ($LD_{50} > 5000$ mg/kg); AOFA, amine oxidase (flavin-containing) A; PGH1, prostaglandin G/H synthase 1.
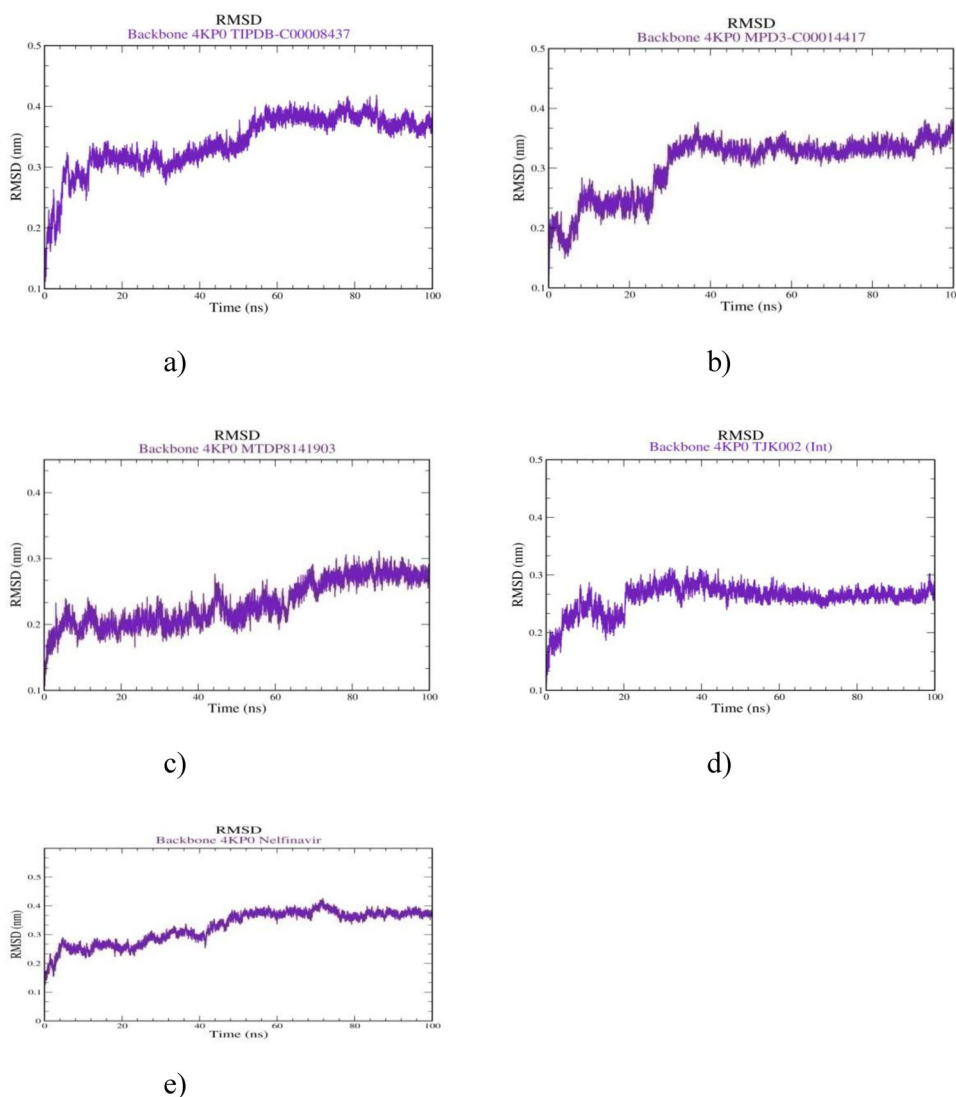
Figure 4. Molecular dynamics (RMSD) for screened ligands (a) C00008437; (b) C00014417; (c) 8141903 and reference compounds; (d) internal ligand; (e) marketed reference-Nelfinavir with chymase receptor.

results were examined with different parameters such as energy, g_rmsd (RMSD), g_rmsf; RMSF (Root Mean Square Fluctuation), g_gyrate (radius of gyration) and % occupancy, respectively.
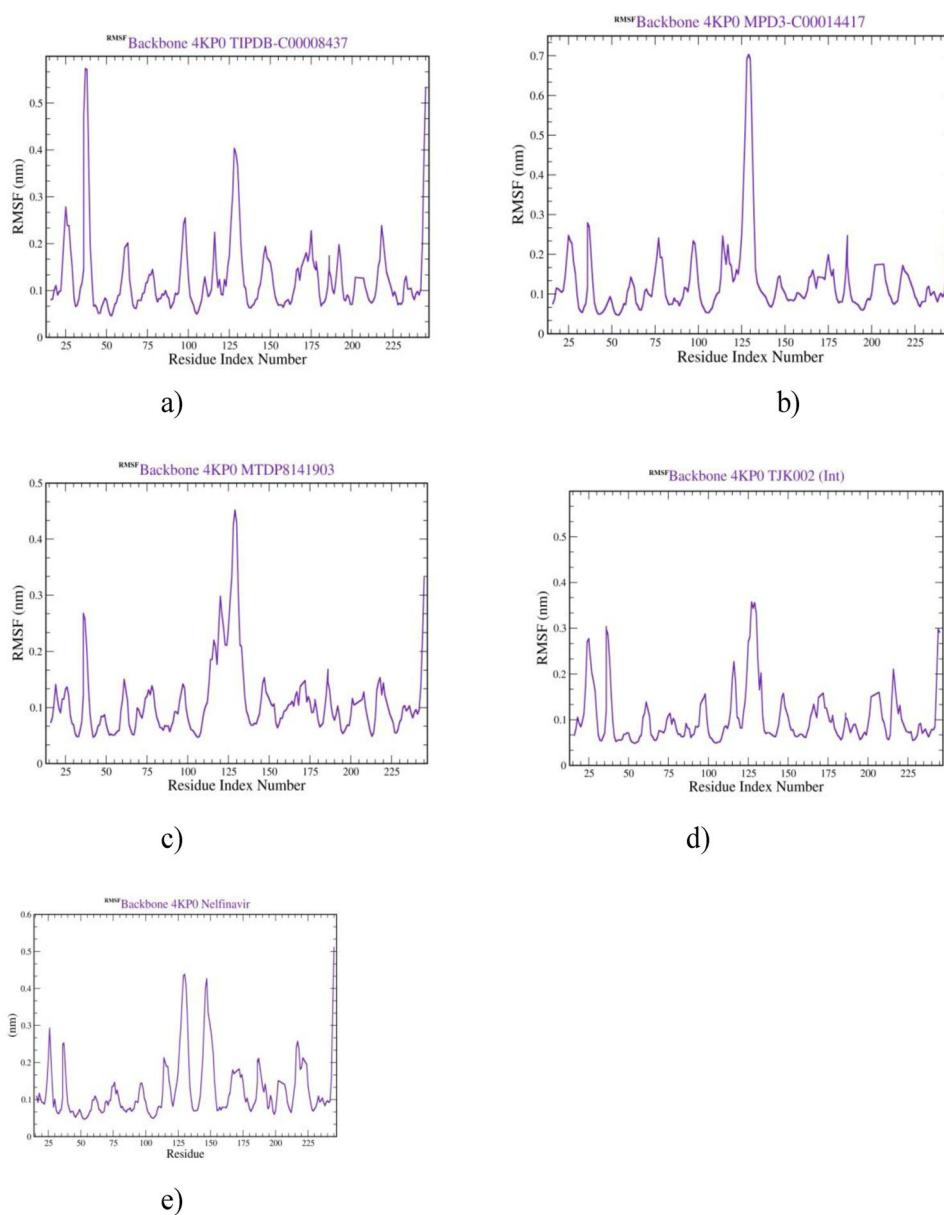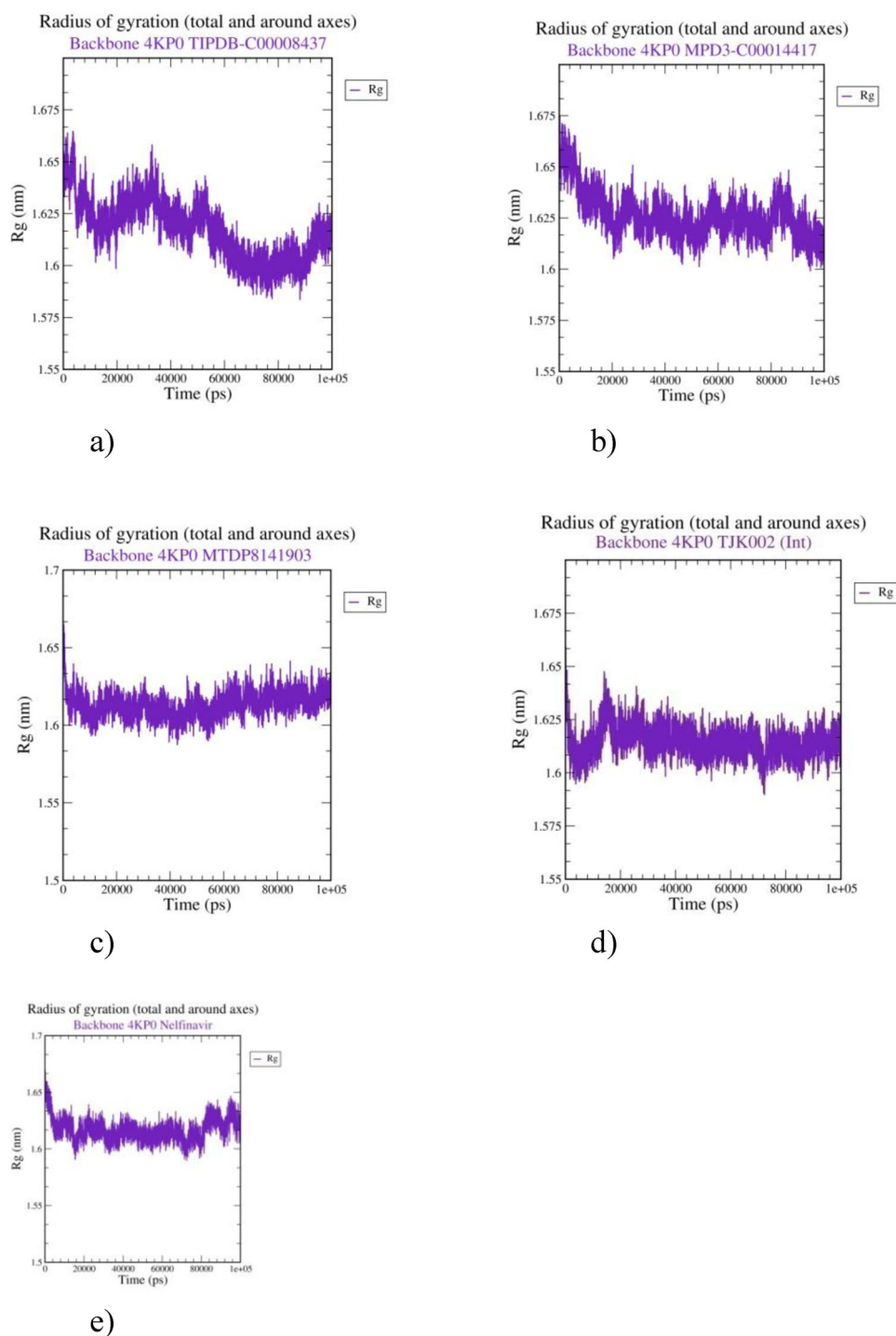
Figure 5. Molecular dynamics (RMSF) for screened ligands (a) C00008437; (b) C00014417; (c) 8141903 and reference compounds; (d) internal ligand; (e) marketed reference-Nelfinavir with chymase receptor.

3. Results and discussion

3.1. Molecular docking and ADME-T analysis

Molecular docking represents the better affinity parameters of tested chemical entities toward targeted receptor, demonstrating a likely lead drug candidate for diseases (Gupta, Kant, Sharma, & Kumar, 2018; Jhanji, Bhati, Singh, & Kumar, 2019). It is the best option to predict the energetically favourable binding conformations of ligands in the active site cavity of particular receptor (Gupta, Kant, et al., 2018). The different natural chemical entity databases (MPD3, MTDP and TIPDB) were docked against human chymase receptor, an important gateway for the pathogenesis of JE infection. The compounds were ranked based on the Gscore and vital ligand interactions such as H- bonding and hydrophobic interactions, respectively. Out of MPD3 (3350), MTDP (106,487) and TIPDB (13,177), apex hits docking poses were

decided. Notably, three modes of docking methods ranged from HTVS, SP and XP were applied. The lower G score values reflect the stronger binding affinity and interaction of apex ligands toward the active site of the human chymase receptor (Supporting Information). Overall, the top three natural chemical entities including C00008437 (TIPDB), C00014417 (MPD3) and 8141903 (MTDP; SID Code) were scrutinized to bind with stronger affinity within the active site of human chymase receptor (Table 1 and supporting information). Interestingly, C00008437 compound attained first rank with a G score of -11.992 kcal/mol followed by notable H-bonding of PHE41, ARG143 and ALA190 while hydrophobic contacts such as PHE41, ALA190, CYS42, PHE191, ALA226, VAL213, TYR215 and LEU99 were displayed with the target receptor (Figure 1 and Table 1). Another compound namely C00014417 resulted as second ranker with significant H-bonding of PHE41, ALA190 and ARG143

a)

b)

c)

d)

e)

Figure 6. Molecular dynamics (radius of gyration) for screened ligands (a) C00008437; (b) C00014417; (c) 8141903 and reference compounds; (d) internal ligand; (e) marketed reference-Nelfinavir with chymase receptor.

(Gscore: −11.673 kcal/mol). Various hydrophobic interactions such as PHE41, CYS42, ALA226, PHE91, ALA190, TYR215 and VAL213 were observed as indicated in Table 1 and Figure 2. Finally, 5459058, compound screened as third hit with a Gscore of −11.456 kcal/mol. The H-bonding interactions like GLY193 and SER195 followed by hydrophobic interactions (PHE41 and TYR215) were well established inside the active site of target receptor (PDB: 4KP0) as shown by Table 1 and Figure 3. Among top hits, C00008437 (first rank) and C00014417 (second rank) showed common H-bonding contact while hydrophobic contact was also almost identical except

additional bonding of PHE191 and LEU99 in case of C00008437 (first rank). However, third ranker compound (8141903) exhibited different H-bonding and hydrophobic amino acid residues contacts when compared with the first and second ranker, respectively. On the other hand, both internal and marketed reference ligands showed less Gscore (internal ligand: Gscoe—4.940/marketed reference: Gscore—6.558 kcal/mol) when compared with tested ligands. Internal ligand (4-({1-[(4-methyl-1-benzothiophen-3-yl)methyl]-1H-benzimidazol-2-yl}sulfanyl)butanoic acid) showed one H-bonding (ALA190) with different hydrophobic contacts such as ALA190, VAL227,

ALA226, VAL213, PHE191, TYR215, LEU99, CYS42 and PHE4, respectively. Moreover, marketed reference (Nelfinavir) exhibited a Gscore of −6.582 kcal/mol with H-bonding (ALA190) and pi-pi interaction (PHE191), correspondingly. Also, the hydrophobic interactions such as ALA190, PHE191, PHE41, ALA220, ALA226, TYR215, VAL213 and Leu99 were monitored (Table 1 and Supporting Information).

Additionally, the top three hits were analyzed for pharmacokinetic and toxicity properties. As poor ADME-T descriptors serve as an important precursor of late-stage letdown in drug development process. For top hits, the ADME-T results revealed an approximately ideal range of descriptor values with small binding behaviour toward Amine oxidase (flavin-containing) A (AOFA) and Prostaglandin G/H synthase 1 (PGH1) targets (Tables 2 and 3).

3.2. Molecular dynamics analysis

As exemplified by molecular docking and ADME-T examinations, the top three hits (C00008437–TIPDB, C00014417-

Table 4. Molecular dynamics H-bonding contact with significant % occupancy of test and reference compounds against chymase receptor residues.

Compounds	Participating amino acid residues (% occupancy)
C00008437 (TIPDB)	ARG217 (26.07)
	PHE41 (19.33)
	GLY216 (10.22)
	ALA190 (6.77)
	ARG143 (6.19)
C00014417 (MPD3)	PHE41 (75.18)
	ARG217(23.62)
	ARG143 (12.93)
	SER218(5.20)
8141903 (MTDP; pubchem SID Code)	ALA209 (9.50)
	ARG143 (7.38)
	GLY201 (6.95)
	ARG27 (6.09)
Marketed reference (Nelfinavir)	ARG174 (57.81)
	GLN180 (50.56)
Internal reference (4-({1-[(4-methyl-1-benzothiophen-3-yl)methyl]-1H-benzimidazol-2-yl}sulfanyl)butanoic acid)	ALA190 (47.23)

MPD3 and 8141903-MTDP) showed strong binding affinity with comparable Gscores toward active pocket of human chymase receptor. To inspect the positive correlation with its molecular docking and ADME-T outcome, the top hits docked complexes with chymase protein were MD simulated for 100 ns. Different trajectories resulted from GROMACS for chymase protein with and without top hits are displayed in Figures 4–6. The top hit docked complexes showed no significant variation of total energy and distribution when compared to apo protein. Also, binding of docked top hits to chymase receptor are displayed over 100 ns of the c-alpha atoms and backbone RMSD bound with and without tested ligands. The fluctuation in the c-alpha atoms and backbone RMSD was observed very less (initial stage) without tested ligands. However, RMSD for chymase bound with first ranked (C00008437) fluctuated little initially for 4–12 ns followed by little crest around 60 ns and ultimately led to significant uniformity for last 100 ns, indicates stability of the system. On the other hand, second (C00014417) and third ranked (8141903) docked top hits showed less fluctuation of RMSD for whole MD run when compared with top docked and reference compounds (Figure 4). Overall, no considerable variation of c-alpha atoms and backbone RMSD were determined between the top hits (docked) bound and targeted chymase protein. Likewise, RMSF was examined to calculate atomic mobility of backbone atoms with structural fluctuation over a period of 100 ns. On the whole, it was observed that molecule specifically C00014417; MPD3) showed less fluctuation when compared with other top docked hits (Figure 5). Initially, it showed identical sensible spike formation between 25–40 and 125–140 residue index numbers as indicated in the apoprotein (backbone) without any tested ligands (Figure 5). An important parameter viz. radius of gyration was further monitored for backbone apoprotein structure and ligands (top hits) bound receptor for 100 ns. In case of apoprotein (without bounded ligands), it showed almost identical behaviour of spikes up to 10,000 ps with little variation around 40,000 ps. On the other hand, top
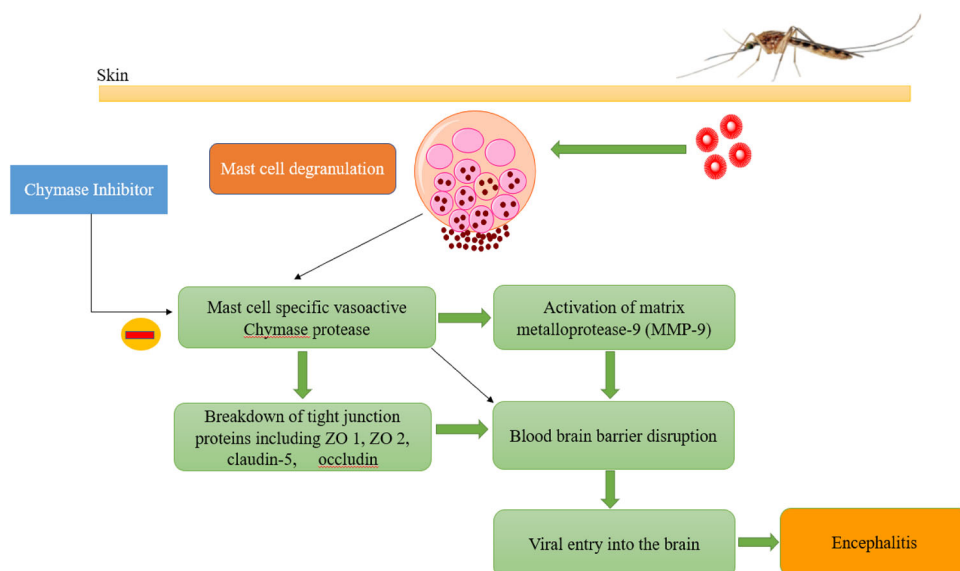
Figure 7. Plausible chymase targeted steps of top screened natural compounds for blocking JEV entry into the brain.

hit (8141903; MTDP) displayed almost steady state behaviour of radius of gyration over an episode of 10,000 ps. However, other apex hits (C00008437; TIPDB and C00014417; MPD3) illustrated low to moderate variation in radius of gyration performance for 10,000 ps (Figure 6). Furthermore, H-bonding contact with worth % occupancy was investigated for test and reference entities against amino acid residues of chymase receptor. The % occupancy was considered at least 5% with amino acid residues of chymase receptor for all top hits chemical entities (Table 4). Ultimately, lead entity (C00014417; MPD3) exhibited highest % occupancy for PHE41 residue (75.18%) when evaluated with other tested compounds. Although, for some tested entities the % occupancy values was ranged from low to moderate but their intactness was well preserved at its active site which signify their significant stability over 100 ns (Table 4).

4. Conclusion and future perspective

This study provided development of natural chemicals as potential inhibitor against human chymase mediated JE infection. For screening, diverse natural product metabolites were screened for the progress of promising and alternative therapy toward JE. Natural product derived database were docked on the active site of chymase receptor (PDB: 4KP0). Following, the best top hits have been selected during meticulous visual scrutiny on the receptor protein employing HTVS, SP and XP molecular docking studies. The selected top hits were further evaluated for drug likeliness and toxicity by inspecting various pharmacokinetic and toxicity parameters. Based on the molecular docking and ADME-T results these ranked compounds were subjected to MD simulation. Ultimately, three top hits (C00008437-TIPDB, C00014417-MPD3 and 8141903-MTDP) were selected by systematically molecular docking assessment via noteworthy Gscore outcome and prominent binding interactions with the target receptor (PDB: 4KP0). The resulted top hits have shown an ideal range of pharmacokinetic descriptors values with allowing limit of toxicity profile and possible targets. Based on the RMSD, RMSF and radius of gyration trajectories of MD simulation, these top hits were confirmed as stable and receptor-ligands remains unaltered. Hydrogen bonding contact for apex hits was further validated to confirm their stability. The stability of top hits was significant for ligand-receptor bonding interactions over a period of 100 ns. Our results displayed an exclusive alternative therapy to combat JEV induced encephalitis. The present outcome insights the probable mechanism mediated through inhibition of mast cell specific chymase protease which further may lead to inactivation of matrix metalloprotease-9 (MMP-9), inhibiting JEV induced breakdown of BBB guided tight junction proteins (ZO-1, ZO-2, Occludin and Claudin-5) and ultimately preventing JEV entry into the brain (Figure 7) (Chen et al., 2014).The present findings conclude that these three top hits can be considered for designing innovative classes of chymase mediated JE inhibitors and further validate them experimentally.

Disclosure statement

No potential conflict of interest was reported by the author(s).

References

Abraham, S., Shwetank, G. K., & Manjunath, R. (2011). Japanese encephalitis virus: Innate and adaptive immunity. In D. Růžek (Ed.), *Flavivirus encephalitis* (pp. 339−382). London, UK: IntechOpen.

Arumugam, K., Subramaniyan, S., Pavulraj, S., Govinthasamy, P., Selvaraj, P., Kannan, P., … Malik, Y. S. (2017). Japanese encephalitis, recent perspectives on virus genome, transmission, epidemiology, diagnosis and prophylactic interventions. *Journal of Experimental Biology and Agricultural Sciences*, 5(6), 730–748. doi:10.18006/2017.5(6).730.748

Bhimaneni, S. P., & Kumar, A. (2020). Abscisic acid, a plant hormone, could be a promising candidate as an anti-Japanese encephalitis virus (JEV) agent. *Anti-Infective Agents*. doi:10.2174/2211352518666200108092127

Campbell, G. L., Hills, S. L., Fischer, M., Jacobson, J. A., Hoke, C. H., Hombach, J. M., … Ginsburg, A. S. (2011). Estimated global incidence of Japanese encephalitis: A systematic review. *Bulletin of the World Health Organization*, 89(10), 766–774. doi:10.2471/BLT.10.085233

Chen, C. J., Ou, Y. C., Li, J. R., Chang, C. Y., Pan, H. C., Lai, C. Y., … Chang, C. J. (2014). Infection of pericytes in vitro by Japanese encephalitis virus disrupts the integrity of the endothelial barrier. *Journal of Virology*, 88(2), 1150–1161. doi:10.1128/JVI.02738-13

Drwal, M. N., Banerjee, P., Dunkel, M., Wettig, M. R., & Preissner, R. (2014). ProTox: A web server for the in silico prediction of rodent oral toxicity. *Nucleic Acids Research*, 42(W1), W53–W58. doi:10.1093/nar/gku401

Ghosh, D., & Basu, A. (2009). Japanese encephalitis—A pathological and clinical perspective. *PLoS Neglected Tropical Diseases*, 3(9), e437. doi:10.1371/journal.pntd.0000437

Gupta, M., Kant, K., Sharma, R., & Kumar, A. (2018). Evaluation of in silico anti-Parkinson potential of β-asarone. *Central Nervous System Agents in Medicinal Chemistry*, 18(2), 128–135. doi:10.2174/1871524918666180416153742

Gupta, M., Sharma, R., & Kumar, A. (2018). Docking techniques in pharmacology: How much promising? *Computational Biology and Chemistry*, 76, 210–217. doi:10.1016/j.compbiolchem.2018.06.005

Halgren, T. A., Murphy, R. B., Friesner, R. A., Beard, H. S., Frye, L. L., Pollard, W. T., & Banks, J. L. (2004). Glide: A new approach for rapid, accurate docking and scoring. 2. Enrichment factors in database screening. *Journal of Medicinal Chemistry*, 47(7), 1750–1759. doi:10.1021/jm030644s

Hills, S. L., Walter, E. B., Atmar, R. L., Fischer, M., ACIP Japanese Encephalitis Vaccine Work Group, ACIP Japanese Encephalitis Vaccine Work Group, … Bocchini, A. (2019). Japanese encephalitis vaccine: Recommendations of the advisory committee on immunization practices. *MMWR Recommendations and Reports*, 68(2), 1–33. doi:10.15585/mmwr.rr6802a1

Hsieh, J. T., Rathore, A. P., Soundarajan, G., & John, A. L. S. (2019). Japanese encephalitis virus neuropenetrance is driven by mast cell chymase. *Nature Communications*, 10(1), 706. doi:10.1038/s41467-019-08641-z

Ioakimidis, L., Thoukydidis, L., Mirza, A., Naeem, S., & Reynisson, J. (2008). Benchmarking the reliability of QikProp. Correlation between experimental and predicted values. *QSAR & Combinatorial Science*, 27(4), 445–456. doi:10.1002/qsar.200730051

Jacob, K. S., Ganguly, S., Kumar, P., Poddar, R., & Kumar, A. (2017). Homology model, molecular dynamics simulation and novel pyrazole analogs design of *Candida albicans* CYP450 lanosterol 14

α-demethylase, a target enzyme for antifungal therapy. *Journal of Biomolecular Structure and Dynamics*, *35*(7), 1446–1463. doi:10.1080/07391102.2016.1185380

Jhanji, R., Bhati, V., Singh, A., & Kumar, A. (2019). Phytomolecules against bacterial biofilm and efflux pump: An in silico and in vitro study. *Journal of Biomolecular Structure and Dynamics*. doi:10.1080/07391102.2019.1704884

Johnson, R. T., Burke, D. S., Elwell, M., Leake, C. J., Nisalak, A., Hoke, C. H., & Lorsomrudee, W. (1985). Japanese encephalitis: Immunocytochemical studies of viral antigen and inflammatory cells in fatal cases. *Annals of Neurology*, *18*(5), 567–573. doi:10.1002/ana.410180510

Kant, K., Lal, U. R., Kumar, A., & Ghosh, M. (2019). A merged molecular docking, ADME-T and dynamics approaches towards the genus of Arisaema as herpes simplex virus type 1 and type 2 inhibitors. *Computational Biology and Chemistry*, *78*, 217–226. doi:10.1016/j.compbiolchem.2018.12.005

Kant, K., Walia, M., Agnihotri, V. K., Pathania, V., & Singh, B. (2013). Evaluation of antioxidant activity of *Picrorhiza kurroa* (leaves) extracts. *Indian Journal of Pharmaceutical Sciences*, *75*(3), 324–329. doi:10.4103/0250-474X.117438

Khalil, M., Ronda, J., Weintraub, M., Jain, K., Silver, R., & Silverman, A. J. (2007). Brain mast cell relationship to neurovasculature during development. *Brain Research*, *1171*, 18–29. doi:10.1016/j.brainres.2007.07.034

Kulkarni, R., Sapkal, G. N., Kaushal, H., & Mourya, D. T. (2018). Suppl-2, M8: Japanese encephalitis: A brief review on Indian perspectives. *The Open Virology Journal*, *12*(1), 121–130. doi:10.2174/1874357901812010121

Kumar, A., Behera, P. C., Rangra, N. K., Dey, S., & Kant, K. (2018). Computational tool for immunotoxic assessment of pyrethroids toward adaptive immune cell receptors. *Pharmacognosy Magazine*, *14*(53), 124–128. doi:10.4103/pm.pm_62_17

Li, F., Wang, Y., Yu, L., Cao, S., Wang, K., Yuan, J., … Fu, Z. F. (2015). Viral infection of the central nervous system and neuroinflammation precede blood-brain barrier disruption during Japanese encephalitis virus infection. *Journal of Virology*, *89*(10), 5602–5614. doi:10.1128/JVI.00143-15

Liu, T. H., Liang, L. C., Wang, C. C., Liu, H. C., & Chen, W. J. (2008). The blood-brain barrier in the cerebrum is the initial site for the Japanese encephalitis virus entering the central nervous system. *Journal of Neurovirology*, *14*(6), 514–521. doi:10.1080/13550280802339643

Lv, B. M., Tong, X. Y., Quan, Y., Liu, M. Y., Zhang, Q. Y., Song, Y. F., & Zhang, H. Y. (2018). Drug repurposing for Japanese encephalitis virus infection by systems biology methods. *Molecules*, *23*(12), 3346. doi:10.3390/molecules23123346

McNaughton, H., Singh, A., & Khan, S. A. (2018). An outbreak of Japanese encephalitis in a non-endemic region of north-east India. *Journal of the Royal College of Physicians of Edinburgh*, *48* (1), 25–29. doi:10.4997/JRCPE.2018.105

Rana, R., Sharma, R., & Kumar, A. (2019). Repurposing of Fluvastatin against *Candida albicans* CYP450 lanosterol 14 α-demethylase, a target enzyme for antifungal therapy: An in silico and in vitro study. *Current Molecular Medicine*, *19*(7), 506–524. doi:10.2174/1566524019666190520094644

Solomon, T., Dung, N. M., Kneen, R., Gainsborough, M., Vaughn, D. W., & Khanh, V. T. (2000). Japanese encephalitis. *Journal of Neurology, Neurosurgery & Psychiatry*, *68*(4), 405–415. doi:10.1136/jnnp.68.4.405

Van Der Spoel, D., Lindahl, E., Hess, B., Groenhof, G., Mark, A. E., & Berendsen, H. J. (2005). GROMACS: Fast, flexible, and free. *Journal of Computational Chemistry*, *26*(16), 1701–1718. doi:10.1002/jcc.20291